V.A. Romaka[1,2], Yu.V. Stadnyk[3], P. Rogl[4], V.V. Romaka[2], V.Ya. Krayovsky[2], O.I. Lakh[5], A.M. Horyn[3]

[1] Ya. Pidstryhach Institute for Applied Problems of Mechanics and Mathematics National Academy of Sciences of Ukraine, 3-b, Naukova Str., Lviv, 79060, Ukraine;

[2] National University "Lvivska Polytechnika", 12, S. Bandera Str., Lviv, 79013,Ukraine;

[3] Ivan Franko National University of Lviv, 6, Kyryla and Mefodiya Str., 79005, Lviv, Ukraine;

[4] Institut für Physikalische Chemie, Universität Wien, Wien, A-1090, Austria;

[5] V.I. Lakh NVO "Termoprylad", 3, Naukova Str., 79060, Lviv, Ukraine;

PARAMETER OPTIMIZATION OF THERMOELECTRIC MATERIAL BASED ON *n-ZrNiSn* INTERMETALLIC SEMICONDUCTOR

The structural, energy, electrokinetic and magnetic characteristics of intermetallic n-ZrNiSn semiconductor heavily doped with Ni impurity are investigated. A new method for parameter optimization of thermoelectric material based on n-ZrNiSn using peculiarities of its crystalline structure is proposed. The mechanism for accumulation in the tetrahedral voids of ZrNiSn compound of both intrinsic and impurity excess atoms generating previously unknown energy levels in the semiconductor is established. It is shown that the obtained thermoelectric material (Zr$_{1-y}$Ni$_y$)Ni$_{1+x}$Sn has high efficiency of thermal into electric energy conversion in the range of investigated temperatures.

Key words: crystal and electronic structures, semiconductor, conduction.

Introduction

It is known that parameter optimization of thermoelectric materials to obtain maximum values of thermoelectric figure of merit Z depends on a series of factors, in particular, current carrier concentration, scattering mechanisms, thermal conductivity, the choice of crystallographic orientation, etc. [1]. Therefore, it is precisely these factors that formed the basis for an algorithm of a new method for parameter optimization of thermoelectric material based on intermetallic *n-ZrNiSn* semiconductor proposed below.

Analyzing the results of studies on *n-ZrNiSn* semiconductor, as well as thermoelectric materials on its basis in various research centres [2-6], we have revealed the presence of essential differences (orders of magnitude) in parameter values under identical temperatures, in particular, electric conductivity, the Seebeck coefficient, thermal conductivity and magnetic susceptibility. Since the purity of precursor components of *ZrNiSn* compound is almost the same in all research laboratories and synthesis methods are also similar, then what is it that provokes the irreproducibility of *n-ZrNiSn* characteristics and virtually eliminates it from the range of materials that can be used for thermal into electric energy conversion?

In the present work, we have not only found the reason for such behaviour of *n-ZrNiSn* characteristics, but on the basis of identified solutions we propose a new method for parameter optimization of thermoelectric material based on *n-ZrNiSn* semiconductor, using the established features of its crystalline and electronic structures. It was preceded by the following reasoning.

1. We proceeded from the assumption that semiconductor properties are largely determined by

the concentration and type of impurities, as well as the depth of their occurrence and the concentration ratio of acceptors and donors (compensation degree) [7]. Therefore, structural defects of *n-ZrNiSn* were analyzed as one of the sources of semiconductor impurity states. Thus, in [6] it was established that crystalline structure of *ZrNiSn* compound is disordered, i.e. crystallographic position of *Zr* ($4d^2 5s^2$) atoms up to~ 2 at.% ($y \leq 0.02$) is occupied with *Ni* ($3d^8 4s^2$) atoms which generates donor-nature structural defects and makes the semiconductor heavily doped and compensated [7]. Precisely this "self-doping" or "a priori doping" method [8] assures the electron type of semiconductor conductivity. In the presence of this structural defect, the compound formula is transformed and has the form of ($Zr_{1-y}Ni_y$)*NiSn*. Besides, it was established that under certain conditions, in particular, on introducing the atoms of rare-earth metals into *ZrNiSn* compound, its structure is arranged in an ordered fashion, i.e. the smallest-size *Ni* atoms ($r_{Ni} = 0.125$ nm) return from *Zr* position ($r_{Zr} = 0.160$ nm) to position of their own [6].

2. Analyzing phase equilibrium diagram of *Zr-Ni-Sn* system, we noticed that alongside with *ZrNiSn* compound (structural type *MgAgAs*, space group $F\overline{4}3m$), there is *ZrNi₂Sn* compound (structural type *MnCu₂Al*, space group $Fm\overline{3}m$). Moreover, it turned out that crystalline structures of the above compounds are related [9]. The difference in them lies in the fact that in *ZrNiSn* compound coordination of *Ni* atoms around *Sn* atoms is tetrahedral, whereas in *ZrNi₂Sn* it is octahedral. The absence of symmetry centre in *ZrNiSn* is caused by the presence of strong tetrahedral covalent bonds between atoms which, on the one hand, is a guarantee of semiconductor compound properties, and, on the other hand, creates in the unit cell a volume making ~ 24 % from the total one which is unoccupied with atoms (the tetrahedral void) (Fig. 1).

By the "relationship" crystallographers mean the following. If we assume hypothetically that the smallest-size *Ni* atoms can be arranged in the tetrahedral voids of *ZrNiSn* and consider a void as a vacancy (*Vac*) of crystallographic position 4*d*, then occupation by *Ni* atom of 4*d* position (vacancy occupation) will result in a change of crystal symmetry and realization under certain *Ni* concentrations of *ZrNi₂Sn* compound.

Based on the relationship between crystalline structures of *ZrNiSn* and *ZrNi₂Sn* compounds, we asked ourselves the following questions:

a) can *Ni* atoms in *ZrNiSn* compound, apart from being arranged in their own crystallographic position and partially (up to 2 at.%) in *Zr* position [6], not hypothetically, but virtually occupy the tetrahedral voids of *ZrNiSn* crystalline structure, generating thereby the earlier unknown structural defects which will result in the redistribution of semiconductor electron density and change its properties? In other words, can tetrahedral voids available in the structure act as traps and accumulate both the excess atoms of *ZrNiSn* compound components and other controlled or uncontrolled impurity atoms?

b) if a certain number of atoms, say, *Ni*, is accumulated in the tetrahedral void of *ZrNiSn,* is the resulting structural defect of a donor, acceptor or neutral nature?

в) how many excess atoms of the smallest-size *Ni* can be accumulated in the unit cell of a semiconductor, without changing its crystalline structure?

Below, based on the results of experimental studies and theoretical calculations, we will show that in *ZrNiSn* compound *Ni* atoms can simultaneously occupy both their own crystallographic position and partially position of *Zr* atoms [6], as well as be arranged in the tetrahedral voids of compound crystalline structure (Fig. 1), generating the earlier unknown donor-nature structural defects. In other words, a situation is created when the excess number of Ni_{1+x} atoms is accumulated in *ZrNiSn* crystal, and compound formula is ($Zr_{1-y}Ni_y$)Ni_{1+x}*Sn*. With a certain number of excess *Ni* atoms,

another $ZrNi_2Sn$ compound is formed. It is precisely the mechanism of accumulation in the tetrahedral voids of $ZrNiSn$ compound of both excess and impurity atoms that generates new energy levels in the semiconductor accounting for the characteristics irreproducibility of n-$ZrNiSn$ synthesized in various research centres [2-6].
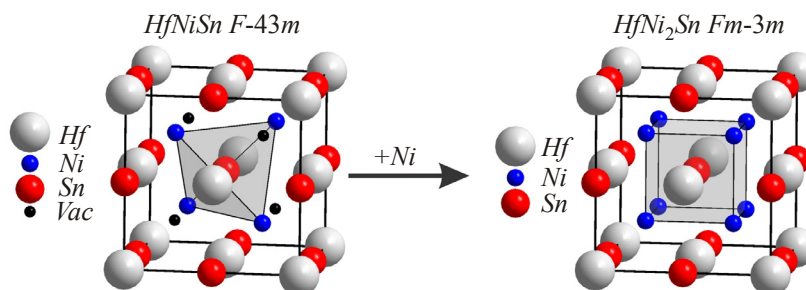

Fig. 1. Transformation of crystalline structure of ZrNiSn compound
in ZrNi₂Sn while accumulating excess Ni_{1+x} atoms in the tetrahedral voids
(occupation of vacant positions by Ni atoms).

Note that our new method of doping n-$ZrNiSn$ semiconductor with Ni donor impurity meets the condition of getting maximum values of thermoelectric power factor [10].

Research methods

The object to be investigated included crystalline structure, electron density distribution (DOS), electrokinetic, magnetic and energy characteristics of $(Zr_{1-y}Ni_y)Ni_{1+x}Sn$. The samples were synthesized in the laboratory of Institute for Physical Chemistry, Vienna University. Structural studies were performed for samples of composition $(Zr_{1-y}Ni_y)Ni_{1+x}Sn$, $x = 0 \div 1.0$ and electrokinetic and magnetic – for $x = 0 \div 0.10$. The *X*-ray structural analysis method was used to obtain the values of $(Zr_{1-y}Ni_y)Ni_{1+x}Sn$, $x = 0 \div 0.10$ crystal lattice periods and to establish its parameters: atom coordinates, thermal parameters and occupancy of crystallographic positions [11]. The data arrays obtained by powder method with a stepwise recording of Bragg reflections intensity were used (diffractometer Guinier-Huber image plate system, $CuK\alpha_1$-radiation; $8° \le 2\theta \le 100°$). Calculations related to interpretation and refinement of $(Zr_{1-y}Ni_y)Ni_{1+x}Sn$ crystalline structure were made with the use of WinCSD program [12]. The phase and chemical compositions were controlled by scanning electron microscope (SEM, Zeiss Supra 55VP) and microprobe analyzer (EPMA, energy-dispersive *X*-ray analyzer). The calculation of DOS was made by KKR-CPA-LDA method (AkaiKKR program [13]). The temperature and concentration dependences of the electrical resistivity ρ, the Seebeck coefficient α and magnetic susceptibility χ of $(Zr_{1-y}Ni_y)Ni_{1+x}Sn$ were measured in the ranges: $T = 80 \div 400$ K, $N_D^{Ni} \approx 9.5 \cdot 10^{19}$ cm^{-3} $(x = 0.005 \div 0.1) \div 1.9 \cdot 10^{21}$ cm^{-3} and magnetic field intensity $H \le 10$ kgf.

Research on $(Zr_{1-y}Ni_y)Ni_{1+x}Sn$ crystalline structure

X-ray phase and structural analyses have shown that the investigated samples of $(Zr_{1-y}Ni_y)Ni_{1+x}Sn$, $0 \le x \le 0.30$ and $0.65 \le x \le 1.0$ are single-phase, *X*-ray diffractograms are indexed in *MgAgAs* and *MnCu₂Al* structural types, respectively, and Bragg R_{Br} factor of a discrepancy between crystalline structure model and the experimental results of structural studies does not exceed 1 % (Table). The composition of semiconductor solid solution $(Zr_{1-y}Ni_y)Ni_{1+x}Sn$, $x \le 0.30$, fixes the solubility limit of *Ni* atoms in the

structure of *ZrNiSn* compound. At the same time, samples of compositions $(Zr_{1-y}Ni_y)Ni_{1+x}Sn$, $0.30 \leq x \leq 0.65$ are not single-phase, pointing to the absence of a continuous solid solution between *ZrNiSn* and *ZrNi₂Sn* compounds.

Table

Structural and metallographic characteristics of $ZrNi_{1+x}Sn$, $(0 \leq x \leq 1)$

Compound composition	$ZrNi_{1+x}Sn$ $(0 \leq x \leq 0.3)$		$ZrNi_{1+x}Sn$ $(0.65 \leq x \leq 1)$
Space group	$F\bar{4}3m$, *MgAgAs*		$Fm\bar{3}m$, *MnCu₂Al*
Composition (SEM), at. %	$Zr_{32.5}Ni_{35.5}Sn_{32.5}$	$Zr_{31.5}Ni_{37.5}Sn_{31.0}$	$Zr_{27.5}Ni_{46.7}Sn_{27.0}$
Composition (EPMA), at.%	$Zr_{33.1}Ni_{33.8}Sn_{33.1}$	$Zr_{33.0}Ni_{34.0}Sn_{33.0}$	$Zr_{25.6}Ni_{48.9}Sn_{25.6}$
a (nm)	0.611173(2)	0.611081(3)	0.627252(7)
R_{Br} (%)	0.0084	0.0069	0.0172
Atom parameters:			
Zr in $4a$ (0, 0, 0)	–	–	–
B_{iso} (10^2 nm²)	0.92(4)	0.57(6)	0.41(11)
Sn in $4b$ (1/2, 1/2, ½)	–	–	–
B_{iso} (10^2 nm²)	0.36(3)	0.38(5)	0.54(9)
Ni in position:	$4d$ (3/4, 3/4, 3/4)	$8c$ (1/4, 1/4, 1/4)	Ni in position:
$Ni/Vac.$	0.09/3.91	0.13/3.87	$Ni/Vac.$
B_{iso} (10^2 nm²)	0.86(4)	0.87(5)	B_{iso} (10^2 nm²)
Ni in $4c$ (1/4, 1/4, 1/4)	–	–	Ni in $4c$ (1/4, 1/4, 1/4)
B_{iso} (10^2 nm²)	0.86(4)	0.87(5)	B_{iso} (10^2 nm²)

The fact that the investigated samples comprise an excess number of Ni_{1+x} atoms whose concentration corresponds to the composition of input components charge mixture is empirically supported by the results of measuring concentration of *Ni* atoms on the surface of samples (Table). In so doing, which is of principal importance, the spatial relationship of atoms in the basic array of compound compositions $(Zr_{1-y}Ni_y)Ni_{1+x}Sn$, $0 \leq x \leq 0.30$ and $0.65 \leq x \leq 1.0$, is not changed. This is indicated by the low values of R_{Br} factor of a discrepancy between the experimental results and the model arrangement of atoms in a space typical of structural types *MgAgAs* and *MnCu₂Al* (Table).

As long as we are interested in *ZrNiSn* compound, it is reasonable to ask: where are Ni_{1+x} excess atoms accumulated in $(Zr_{1-y}Ni_y)Ni_{1+x}Sn$, $0 \leq x \leq 0.30$, and what is the nature of structural defects generated thereby which define the semiconductor properties?

The refinement of crystalline structure of $(Zr_{1-y}Ni_y)Ni_{1+x}Sn$, $0 \leq x \leq 0.30$ samples has shown that when excess Ni_{1+x} atoms are arranged in crystallographic position $4d$ (the tetrahedral void), the discrepancy factor does not exceed 0.8 %, which is even slightly incorrect, since it exceeds the accuracy of the measuring system. Thus, doping of *n-ZrNiSn* semiconductor with *Ni* atoms results in the formation of point structural defects – *Ni* atoms in the interstitial site (the tetrahedral voids), the type of which will be established from the results of calculating the semiconductor electron structure

and the electrokinetic properties.

The refinement of crystalline structure of samples also allowed establishing an important result which in the future will help to identify the type of defects that are generated in the crystal. It turned out that doping of *n-ZrNiSn* with *Ni* atoms is accompanied by ordering semiconductor crystalline structure through return of Ni_y atoms from *Zr* crystallographic position to their own crystallographic position (Fig. 2). If we take into account that exactly Ni_y atoms, partially occupying *Zr* crystallographic position, generate donor-nature structural defects in the crystal, then ordering of crystalline structure on introduction of excess Ni_{1+x} atoms will be accompanied by a decrease in donor concentration ("healing" of donor-nature structural defects). As can be seen from Fig. 2, at concentration of excess Ni_{1+x} atoms that corresponds to compositions $(Zr_{1-y}Ni_y)Ni_{1+x}Sn$, $x \geq 0.07$, there are no donor-nature structural defects in the crystal that are related to "a priori doping" of a semiconductor.
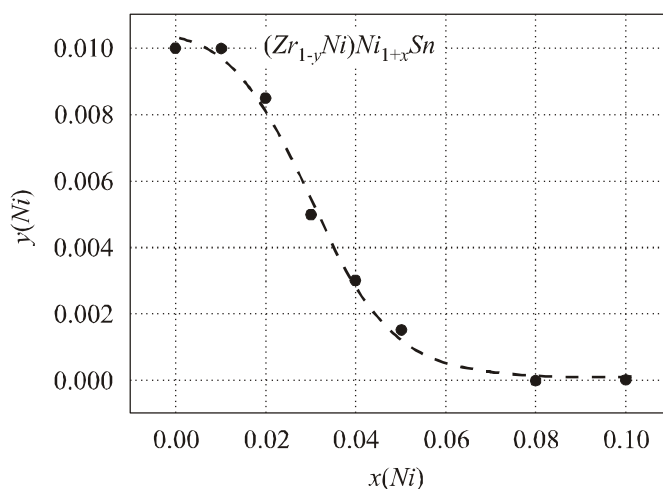

Fig. 2. Dynamics of change in the concentration of Ni_y atoms
in Zr crystallographic position $(Zr_{1-y}Ni_y)Ni_{1+x}Sn$, $x \leq 0.10$.

Thus, structural studies of *n-ZrNiSn* heavily doped with *Ni* atoms have confirmed the above assumption that crystal can accumulate an excess amount of Ni_{1+x} atoms in the tetrahedral voids. In so doing, in a semiconductor there takes place a dynamic change in the compensation degree which reduces the concentration of donor-nature defects related to a reduced amount of donor-nature structural defects (Ni_y atoms in *Zr* position). At the same time, structural studies cannot identify the nature of defects that arose while accumulating Ni_{1+x} atoms in the semiconductor tetrahedral voids.

Research on electron density distribution in $(Zr_{1-y}Ni_y)Ni_{1+x}Sn$

To predict the behaviour of the Fermi level ε_F, the energy gap ε_g, the electrokinetic and magnetic characteristics of *n-ZrNiSn* doped with *Ni* atoms, the electron density distribution was calculated with regard to the contribution of Ni_{1+x} excess atoms located in the tetrahedral voids of semiconductor structure. Taking into consideration that introduction of excess Ni_{1+x} atoms into *ZrNiSn* compound arranges in an ordered fashion its crystalline structure, calculation of DOS was carried out for the case of ordered crystalline structure. Introduction of excess Ni_{1+x} atoms into concentrations of $(Zr_{1-y}Ni_y)Ni_{1+x}Sn$, $0 \leq x \leq 0.30$, does not radically change the shape of electron density distribution in conformity to hybridization between all the elements (Fig. 3). There is an increase in the "tails" of continuous energy bands, leading to a slight reduction in the values of efficient energy gap (Fig. 4 *a*, insert) in $(Zr_{1-y}Ni_y)Ni_{1+x}Sn$.
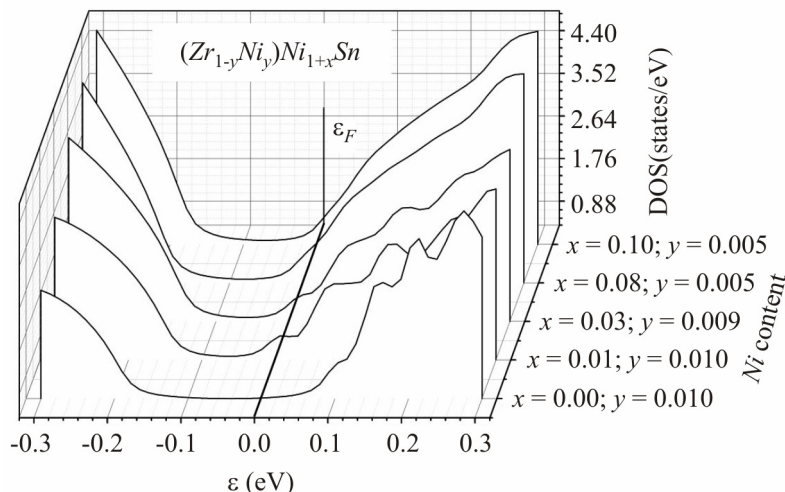
Fig. 3. Calculation of change in the edge profiles of continuous energy bands in $(Zr_{1-y}Ni_y)Ni_{1+x}Sn$.

As is evident from Fig. 4 *b*, with an increase in concentration of Ni_{1+x} atoms, the density of states on the Fermi level $DOS\varepsilon_F$ in $(Zr_{1-y}Ni_y)Ni_{1+x}Sn$ is also increased, and the Fermi level moves in the direction of conduction band (Fig. 4 *a*, dependence 1). In a semiconductor, this is possible only on condition of its doping with donor impurity. Note that the results of calculating the position of the Fermi level relative to the edge of conduction band in $Zr_{1-y}Ni_y)Ni_{1+x}Sn$ are of a more complicated character than a regular drift due to the effect of electron-type Ni donor impurity introduced into a semiconductor. Apart from the drift caused by a reduction in semiconductor compensation degree, there is also a reduction in the values of effective energy gap ε_g from ε_g $(x = 0) = 287.7$ meV to ε_g $(x = 0.01) = 181.7$ meV due to increase in band "tails" changing the profile of continuous energy bands (Fig. 4 *a*, insert).
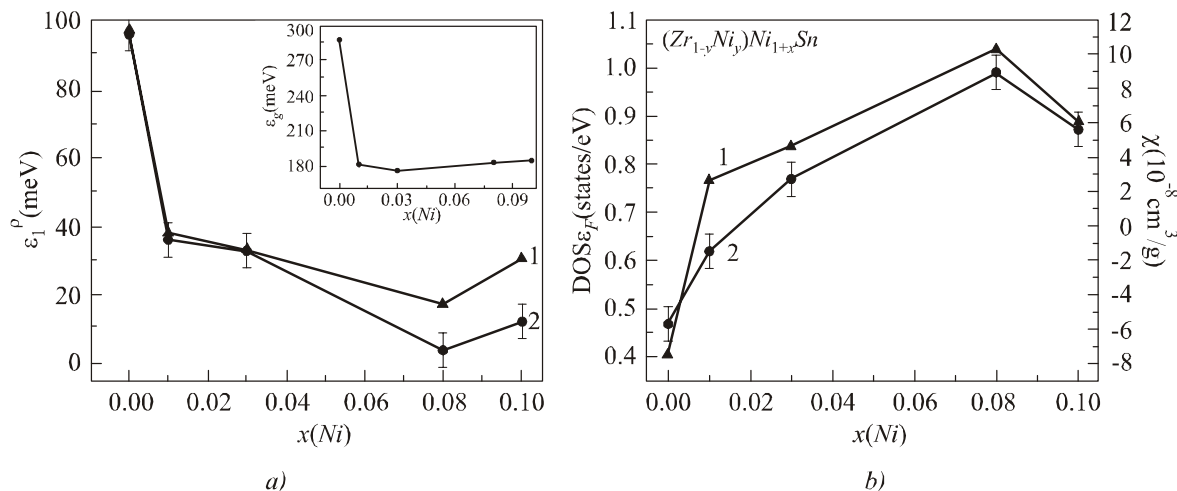

a)

b)

Fig. 4. A change in the values of activation energy ε_1^ρ from the Fermi level to percolation level of conduction band (a): 1 – from $\ln\rho(1/T)$ dependences; 2 – calculation; insert – energy gap ε_g and density of states on the Fermi level $DOS\varepsilon_F$ (1), magnetic susceptibility χ (2) at T = 300 K, (b) $(Zr_{1-y}Ni_y)Ni_{1+x}Sn_x$.

Thus, the results of calculation of electron density distribution in $(Zr_{1-y}Ni_y)Ni_{1+x}Sn_x$ based on the results of structural research point to a donor nature of generated structural defects, and experimental studies will allow checking the adequacy of calculation results, hence of selected model of semiconductor structure.

Research on the magnetic characteristics of $(Zr_{1-y}Ni_y)Ni_{1+x}Sn$

Research on the field and temperature dependences of magnetic susceptibility χ $(Zr_{1-y}Ni_y)Ni_{1+x}Sn$ provided additional information as to the reasons for a change in the electronic structure of a semiconductor. Fig. 4 *b* shows the results of measuring $\chi(x)$ values at $T = 300$ K and magnetic field intensity $H = 10$ kgf. The *n-ZrNiSn* is known to be a weak diamagnetic ($\chi_{x=0} = -0.057 \cdot 10^{-6}$ cm³/g) [8]. Introduction of weak concentrations of Ni_{1+x} atoms reduces the diamagnetic component $\chi_{x=0.01} = -0.015 \cdot 10^{-6}$ cm³/g, and with the concentration $x \geq 0.03$ the semiconductor becomes the Pauli paramagnetic and $\chi_{x=0.03} = 0.027 \cdot 10^{-6}$ cm³/g. In this case, the magnetic susceptibility $(Zr_{1-y}Ni_y)Ni_{1+x}Sn$ is governed by the major carriers, and its values are proportional to concentration of free electrons n (for the Pauli paramagnetic $\chi \sim n$). Taking into account that $\chi(x)$ dependence in $(Zr_{1-y}Ni_y)Ni_{1+x}Sn$ grows, we can state that donor-nature structural defects are generated in the crystal when the tetrahedral voids are occupied by *Ni* atoms.

Research on the electrokinetic characteristics of $(Zr_{1-y}Ni_y)Ni_{1+x}Sn$

The temperature dependences of electric resistivity $\ln\rho(1/T)$ and the Seebeck coefficient $\alpha(1/T)$ for samples of $(Zr_{1-y}Ni_y)Ni_{1+x}Sn$, $x = 0 \div 0.10$ are represented in Fig. 5 and are typical of doped and compensated semiconductors with high and low-temperature activation regions. Such regions of dependences $\ln\rho(1/T)$ were used to calculate the values of activation energy from the Fermi level ε_F to percolation level of conduction band (ε_1^ρ) and electron hops (ε_3^ρ) in the states with energies close to ε_F, and dependences $\alpha(1/T)$ were used to calculate the values of activation energies ε_1^α and ε_3^α, proportional to modulation amplitude of continuous energy and small-scale fluctuation zones, respectively [14].
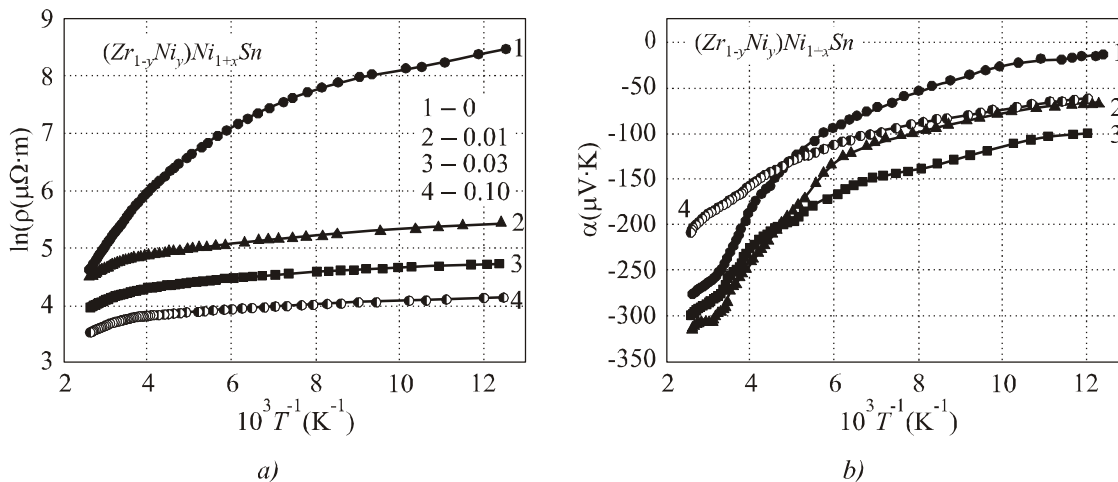

Fig. 5. Temperature dependences of electric resistivity ρ (a) and the Seebeck coefficient α (b)
$(Zr_{1-y}Ni_y)Ni_{1+x}Sn$: 1 – x = 0; 2 – x = 0.01; 3 – x = 0.03; 4 – x = 0.10.

As can be seen from Figs. 5 *b* and 6 *b*, the Seebeck coefficient $(Zr_{1-y}Ni_y)Ni_{1+x}Sn$, $x = 0$, (*n-ZrNiSn*) has negative values, and electrons are major carriers. This is a well-known and expected result which is related to the donor nature of intrinsic structural defects in a semiconductor due to partial occupation by Ni_y atoms of *Zr* crystallographic position ("a priori doping") [6]. In this case, the Fermi level ε_F is located close to the bottom of conduction band at the distance of $\varepsilon_1^\rho(x = 0) = 97.6$ meV from the percolation level, and $\varepsilon_1^\alpha(x = 0) = 83.8$ meV determines the modulation amplitude of continuous energy bands of *n-ZrNiSn* (Fig. 4 *a*).
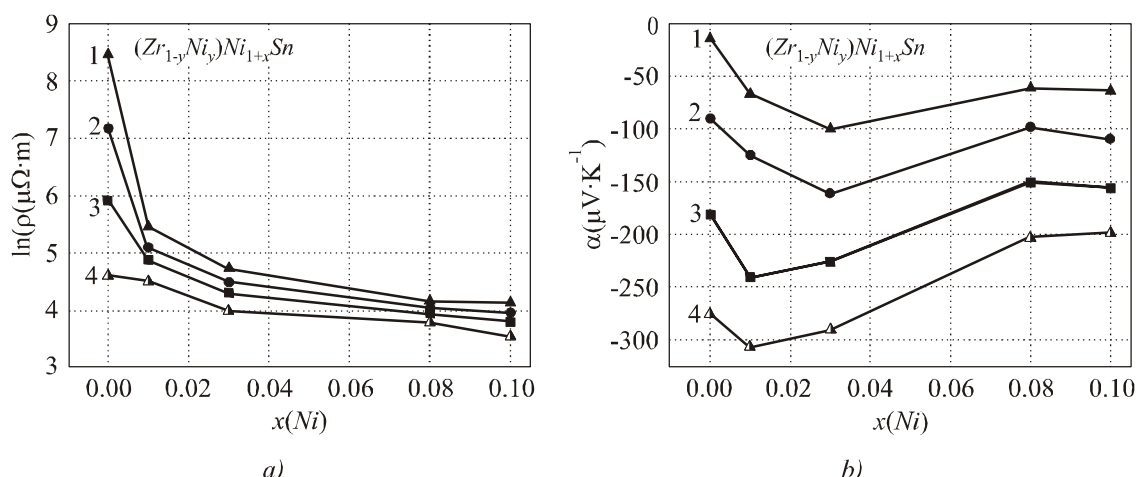
Fig. 6. A change in the values of electric resistivity ρ (a) and the Seebeck coefficient α (b) (Zr$_{1-y}$Ni$_y$)Ni$_{1+x}$Sn at different temperatures: 1 – T = 80 K; 2 – T = 160 K; 3 – T = 250 K; 4 – T = 380 K.

Introduction into *ZrNiSn* compound of the smallest concentrations of *Ni$_{1+x}$* atoms leads to a drastic reduction of electric resistivity values, for instance, at 80 K, from the values of $\rho(x = 0) = 4751.1\ \mu$Ohm·m to $\rho(x = 0.01) = 231.0\ \mu$Ohm·m and $\rho(x = 0.10) = 62.8\ \mu$Ohm·m. Such behaviour of $\rho(x)$ dependence testifies that donor-nature structural defects are created in the crystal whose concentration grows with increasing the content of *Ni$_{1+x}$* atoms. This is regardless of the fact that, as follows from structural studies, introduction of excess *Ni$_{1+x}$* atoms first reduces the number of donor-nature structural defects due to return of *Ni$_y$* atoms from *Zr* position to their own crystallographic position.

Thus, the results of electrokinetic research on (*Zr$_{1-y}$Ni$_y$*)*Ni$_{1+x}$Sn* lead to the conclusion as to the donor type of defects generated in the crystal of *ZrNiSn* compound while introducing excess *Ni$_{1+x}$* atoms and accumulating these atoms in the tetrahedral voids of the structure. In this case, the degree of semiconductor compensation is reduced, and the dependence in Fig. 2 describes the dynamics of change in the number of various types of structural defects of (*Zr$_{1-y}$Ni$_y$*)*Ni$_{1+x}$Sn*.

The fact that donor-nature structural defects are generated in the crystal while introducing excess *Ni$_{1+x}$* atoms is evidenced by the character of the Fermi level drift in the direction of conduction band (Fig. 4 *a*, dependence 1). We can see that introducing the lowest concentrations of excess *Ni$_{1+x}$* atoms into *n-ZrNiSn* is accompanied by a drastic decrease in the values of activation energy ε_1^ρ from the Fermi level to percolation level of conduction band from $\varepsilon_1^\rho(x = 0) = 97.6$ meV to $\varepsilon_1^\rho(x = 0.01) = 38.3$ meV. On the other hand, if the degree of semiconductor compensation is reduced, then it is quite logical that the values of modulation amplitude of continuous energy bands [7] will be reduced to values $\varepsilon_1^\alpha(x = 0.01) = 51.4$ meV and $\varepsilon_1^\alpha(x = 0.10) = 31.9$ meV. Besides, exactly due to this at low temperatures the length of electron hop ε_3^ρ will decrease in the states close to the Fermi energy from the values of $\varepsilon_3^\rho(x = 0) = 11.5$ meV to $\varepsilon_3^\rho(x = 0.01) = 4.4$ meV and $\varepsilon_3^\rho(x = 0.08) = 1.4$ meV. Note that concentration of excess *Ni$_{1+x}$* atoms introduced into *n-ZrNiSn* proved to be insufficient for the intersection by the Fermi level of the percolation level of conduction band and realization of dielectric-metal transition in the conductivity [7].

Thus, the experimentally observed drastic decrease in the values of electric resistivity $\rho(x)$ (Fig. 6 *a*), activation energy $\varepsilon_1^\rho(x)$ from the Fermi level to the percolation level of conduction band (Fig. 4 *a*), as well as the negative values of the Seebeck coefficient $\alpha(x)$ is related both to increased

concentration of donor-nature defects and decreased energy gap between continuous energy bands, which facilitates throwing of electrons from the donor levels to the conduction band of a heavily doped and compensated semiconductor $(Zr_{1-y}Ni_y)Ni_{1+x}Sn$. This statement makes specific the consequence of structural research and confirms that which is based on the results of calculating the semiconductor electronic structure and its magnetic characteristics.

Thermoelectric power factor of $(Zr_{1-y}Ni_y)Ni_{1+x}Sn$

Maximum values of thermoelectric power factor Z^* ($Z^* = \alpha^2\sigma$, where α is the Seebeck coefficient, σ is electric conductivity) are attained under condition when the Seebeck coefficient is still high and the electric conductivity values of $(Zr_{1-y}Ni_y)Ni_{1+x}Sn$ semiconductor solid solution have become even higher [10]. Under these conditions, on $Z^*(x)$ dependences there are extremes at all temperatures under study. Fig. 7 *a* shows $Z^*(x)$ dependence from which it is seen that the value of thermoelectric factor in $(Zr_{1-y}Ni_y)Ni_{1+x}Sn$ is higher than in the undoped semiconductor *n-ZrNiSn*. Besides, with a rise in temperature the absolute values of $Z^*(T)$ are still further increased (Fig. 7 *b*). Taking into account that calculations show a slight (by ~ 5 %) increase of thermal conductivity κ for $(Zr_{1-y}Ni_y)Ni_{1+x}Sn$, $x = 0.03$, the values of thermoelectric figure of merit Z with this impurity concentration will be higher than in the undoped semiconductor *n-ZrNiSn*.
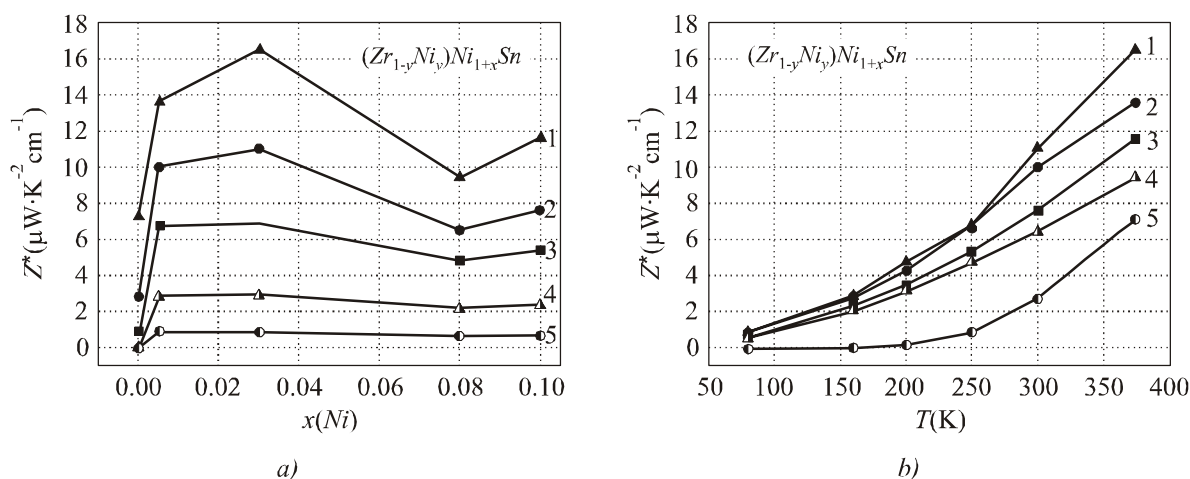

Fig. 7. Changes in the values of thermoelectric power factor Z* ($Zr_{1-y}Ni_y)Ni_{1+x}Sn$
with a change in composition (a): 1 – T = 375 K; 2 – T = 300 K; 3 – T = 250 K;
4 – T = 160 K; 5 – T = 80 K and temperature (b): 1 – x = 0.03;
2 – x = 0.005; 3 – x = 0.10; 4 – x = 0.08; 5 – x = 0.

Conclusions

As a result of integrated research on the crystalline structure, energy spectrum, electrokinetic and magnetic characteristics of intermetallic semiconductor *n-ZrNiSn* heavily doped with a donor impurity *Ni*, the effect of accumulation of excess Ni_{1+x} atoms in the tetrahedral voids of $(Zr_{1-y}Ni_y)Ni_{1+x}Sn$ structure up to concentrations $0 \le x \le 0.30$ has been revealed, and the donor nature of such structural defect has been established. The use of this effect for semiconductor doping is a new mechanism for parameter optimization of thermoelectric material based on *n-ZrNiSn*. It is shown that the obtained thermoelectric material $(Zr_{1-y}Ni_y)Ni_{1+x}Sn$ has high efficiency of thermal into electric energy conversion in the range of investigated temperatures.

V.A. Romaka, Yu.V. Stadnyk, P. Rogl, V.V. Romaka, V.Ya. Krayovsky, O.I. Lakh, A.M. Horyn
Parameter optimization of thermoelectric material based on n-ZrNiSn intermetallic semiconductor

References

1. L.I. Anatychuk, *Thermoelements and Thermoelectric Devices [Handbook]* (Kyiv: Naukova Dumka, 1979), 768 p.

2. T.M. Tritt, Thermoelectric Materials, Phenomena, and Applications: A Bird's Eye View, *MRS Bulletin* **31**, 188 (2006).

3. S.R. Culp, S.J. Poon, N. Hickman, T.M. Tritt, and J. Blumm, Effect of Substitutions on the Thermoelectric Figure of Merit of Half-Heusler Phases at 800 °C, *Appl. Phys. Letters* **88** (16), 042106-1-3 (2006).

4. Y. Kawaharada, H. Uneda, H. Muta, K. Kurosaki, S. Yamanaka, High Temperature Thermoelectric Properties of *NiZrSn* Half-Heusler Compounds, *J. Alloys and Compounds* **364**, 59 (2004).

5. C. Uher, J. Yang, S. Hu, D.T. Morelli, and G.P. Meisner, Transport Properties of Pure and Doped *MNiSn* (*M* = *Zr, Hf*), *Phys. Rev. B* **59** (13), 8615 (1999).

6. V.A. Romaka, D. Fruchart, E.K. Hlil, P.E. Gladyshevsky, D. Gignoux, V.V. Romaka, B.S. Kuzhel, R.V. Krayovsky, Features of *n-ZrNiS*n Intermetallic Semiconductor Heavily Doped with Atoms of Rare-Earth Metals, *Semiconductors* **44** (3), 310 (2010).

7. B.I. Shklovsky, A.L. Efros, *Electronic Properties of Doped Semiconductors* (Moscow: Nauka, 1979), 416 p.

8. V.A. Romaka, V.V. Romaka, and Yu.V. Stadnyk, *Intermetallic Semiconductors: Properties and Appications* (Lviv: Lvivska Politekhnika, 2011), 488 p.

9. R. Ferro and A. Saccone, *Intermetallic Chemistry* (Amsterdam: Elsevier, 2008), 786 p.

10. V.A. Romaka, D. Fruchart, Yu.V. Stadnyk, J. Tobola, Yu.K. Horelenko, M.G. Shelyapina, L.P. Romaka, V.F. Chekurin, Conditions for the Attainment of Maximum Values of Thermoelectric Power Factor in the Intermetallic Semiconductors of *MgAgAs* Structural Type, *Semiconductors* **40** (11), 1309 (2006).

11. V.K. Pecharsky, P.U. Zavalij, *Fundamentals of Powder Diffraction and Structural Characterization of Materials* (New York: Springer, 2005), 713 p.

12. L.G. Akselrud, Yu.N. Grin, P.Yu. Zavalii, V.K. Pecharsky, V.S. Fundamenskii, CSD – Universal Program Package for Single Crystal or Powder Structure Data Treatment, *12 Eur. Crystallogr. Meeting Coll. Abstr., Vol. 3* (Moscow: Nauka, (1989), 155 p.

13. M. Schröter, H. Ebert, H. Akai, P. Entel, E. Hoffmann, G.G. Reddy, First-Principles Investigations of Atomic Disorder Effects on Magnetic and Structural Instabilities in Transition-Metal Alloys, *Phys. Rev. B* **52**, 188 (1995).

14. V.A. Romaka, Yu.V. Stadnyk, V.V. Romaka, D. Fruchart, YU.K. Horelenko, V.F. Chekurin, and A.M.Horyn, Conduction Peculiarities of *n-ZrNiSn* Intermetallic Semiconductor Heavily Doped with In Acceptor Impurity, *Semiconductors* **41** (9), 1059 (2007).